

THE COLD NEUTRON STAR IN THE SOFT X-RAY TRANSIENT 1H 1905+000

PETER G. JONKER^{1,2}

SRON, Netherlands Institute for Space Research, Sorbonnelaan 2, 3584 CA, Utrecht, The Netherlands

DANIEL STEEGHS³

Harvard-Smithsonian Center for Astrophysics, 60 Garden Street, Cambridge, MA 02138, Massachusetts, U.S.A.

DEEPTO CHAKRABARTY

Department of Physics and Kavli Institute for Astrophysics and Space Research, Massachusetts Institute of Technology, Cambridge, MA 02139, U.S.A.

AND

ADRIENNE M. JUETT

Department of Astronomy, University of Virginia, Charlottesville, VA 22903, U.S.A.

Draft version March 28, 2022

ABSTRACT

We report on our analysis of 300 ks of *Chandra* observations of the neutron star soft X-ray transient 1H 1905+000 in quiescence. We do not detect the source down to a 95% confidence unabsorbed flux upper limit of 2×10^{-16} erg cm⁻² s⁻¹ in the 0.5–10 keV energy range for an assumed $\Gamma = 2$ power law spectral model. A limit of 1.4×10^{-16} erg cm⁻² s⁻¹ is derived if we assume that the spectrum of 1H 1905+000 in quiescence is described well with a black body of temperature of 0.2 keV. For the upper limit to the source distance of 10 kpc this yields a 0.5–10 keV luminosity limit of 2.4×10^{30} erg s⁻¹ / 1.7×10^{30} erg s⁻¹ for the abovementioned power law or black body spectrum, respectively. This luminosity limit is lower than the luminosity of A 0620–00, the weakest black hole soft X-ray transient in quiescence reported so far. Together with the uncertainties in relating the mass transfer and mass accretion rates we come to the conclusion that the claim that there is evidence for the presence of a black hole event horizon on the basis of a lower quiescent luminosity for black holes than for neutron stars is unproven. We also briefly discuss the implications of the low quiescent luminosity of 1H 1905+000 for the neutron star equation of state. Using deep Magellan images of the field of 1H 1905+000 obtained at excellent observing conditions we do not detect the quiescent counterpart of 1H 1905+000 at the position of the outburst optical counterpart down to a magnitude limit of $i' > 25.3$. This can be converted to a limit on the absolute magnitude of the counterpart of $I > 9.6$ which implies that the counterpart can only be a brown or a white dwarf.

Subject headings: stars: individual (1H 1905+000) — accretion: accretion discs — stars: binaries — stars: neutron — X-rays: binaries

1. INTRODUCTION

Low-mass X-ray binaries (LMXBs) are binary systems in which a compact object, either a neutron star or a black hole, accretes matter from a companion star that has a mass of typically less than $1 M_{\odot}$. Such systems are excellent test beds for a range of astrophysical questions and probe fundamental physics. Theories, such as Einstein's Theory of General Relativity, can be tested in the strong field regime by comparing the observed black hole and neutron star properties. The presence of an event horizon in the case of a black hole is such a prediction. Observations of neutron star LMXBs can also help constrain the equation of state of matter at supra-nuclear densities encountered in the neutron star core.

Observationally, it was found that in general the luminosity

of quiescent black hole LMXBs is lower than that of quiescent neutron star LMXBs (e.g. Garcia et al. 2001, Kong et al. 2002 and Jonker et al. 2006). However, recent *Chandra* and *XMM-Newton* observations of several transient neutron star LMXBs in quiescence have shown that the luminosities of these sources span a much larger range extending to lower luminosities than previously thought (e.g. Tomsick et al. 2005, Wijnands et al. 2005).

The neutron star transient with the lowest quiescent X-ray luminosity is 1H 1905+000. Using a 25 ks long observation of 1H 1905+000 with the *Chandra* satellite, Jonker et al. (2006) did not detect the source in quiescence down to a luminosity of 1.8×10^{31} erg s⁻¹. This means that the neutron star luminosity in this source is comparable to that of several quiescent black hole LMXBs. For a recent introduction on 1H 1905+000, for a more detailed introduction on the difference in quiescent luminosity between neutron star and black hole LMXBs, and for an explanation why these transient neutron stars in quiescence can provide information on the neutron star equation of state we refer to Jonker et al. (2006) (see also Yakovlev & Pethick 2004 and Heinke et al. 2006 for the latter subject).

In this Letter, we present our analysis of a long *Chandra* and a deep Magellan observation of 1H 1905+000 obtained

Electronic address: p.jonker@srn.nl
Electronic address: dsteeghs@cfa.harvard.edu
Electronic address: deepto@space.mit.edu
Electronic address: amj3r@astsun.astro.virginia.edu

¹ Harvard-Smithsonian Center for Astrophysics, 60 Garden Street, Cambridge, MA 02138, Massachusetts, U.S.A.

² Astronomical Institute, Utrecht University, P.O.Box 80000, 3508 TA, Utrecht, The Netherlands

³ Astronomy & Astrophysics, Department of Physics, University of Warwick, Coventry CV4 7AL, U.K.

TABLE 1
LOG OF THE *Chandra* OBSERVATIONS

ID	T ₀ (UTC)	Exposure ^a (ks)	Boresight corr. (α , δ)
5549	Febr. 25, 2005	24.84	0''128±0''044,-0''074±0''041
6649	Sept. 17, 2006	151.92	0''314±0''018,0''611±0''019
6650	Sept. 20, 2006	40.63	-1''07±0''030,0''047±0''039
8261	Sept. 17, 2006	41.61	-1''08±0''029,0''539±0''033
8262	Sept. 22, 2006	38.65	-0''789±0''025,0''392±0''030
8283	Sept. 19, 2006	3.15	-0''820±0''066,0''758±0''087

^a After taking into account the CCD read-out time and after filtering for flares.

with the aim to detect the source or provide a stringent limit on the source flux and the source luminosity in quiescence.

2. OBSERVATIONS AND ANALYSIS

2.1. *Chandra* X-ray observations

We have observed 1H 1905+000 with the back-illuminated S3 CCD-chip of the Advanced CCD Imaging Spectrometer (ACIS) detector on board the *Chandra* satellite. A log of the observations is given in Table 1. The data telemetry mode was set to *very faint* to allow for a thorough background subtraction. A CCD frame time of 3.04104 s has been used. We have reprocessed and analysed the data using the *CIAO 3.4* software developed by the *Chandra* X-ray Center using CALDB version 3.3.0.1, to benefit from the latest calibrations available early 2007 and to take full advantage of the *very faint* data mode. In our analysis we have selected events only if their energy falls in the 0.3–7 keV range in order to reduce the background contamination that occurs at high energies. The lower cut-off was chosen to avoid calibration uncertainties below 0.3 keV. Since fluxes and luminosities are commonly provided in the 0.5–10 keV range, we extrapolate our 0.3–7 keV event rate to model fluxes over the 0.5–10 keV range in the remainder of this Letter. Data were excluded for which the 0.3–7 keV background count rate is higher than 0.4 counts s⁻¹. The net on-source exposure time is 300.8 ks.

In the observations presented in Table 1 one source (CXOU J190834.1+001139) is always detected (we will describe the properties of detected sources unrelated to 1H 1905+000 or to the presented analysis in a forthcoming paper). The J2000.0 α and δ position of that source was determined in Jonker et al. (2006) to be $\alpha_{J2000.0} = 19^{\text{h}}08^{\text{m}}34^{\text{s}}.108 \pm 0''033$, $\delta_{J2000.0} = +00^{\circ}11'39''.01 \pm 0''032$. We use this source to apply a boresight correction to each of the observations separately (see Table 1) before combining them. In addition we applied a boresight correction of (α , δ)=0''090±0''013,-0''208±0''014 to the final combined image such that the coordinates for CXOU J190834.1+001139 measured on the combined image are, within errors, consistent with the optical coordinates. The latter boresight correction accounts for the limited accuracy with which the source position can be determined in the individual observations.

The outburst position of 1H 1905+000 is $\alpha_{J2000.0} = 19^{\text{h}}08^{\text{m}}27^{\text{s}}.200 \pm 0''084$, $\delta_{J2000.0} = +00^{\circ}10'09''.10 \pm 0''087$ (Jonker et al. 2006). The largest off-axis angle that the source position was observed at was $\theta = 0'.54$ (see Table 1). Using the analytical expression for the 90% encircled energy radius, R_{90} (in $''$)= $0.881 + 0.107\theta^2$ (θ in arc minutes) as given in Murray (2005), this leads to a 90% encircled energy radius of $R_{90}=0''.91$. Less than two photons have been detected in the circular area spanned by R_{90} (see Figure 1). From the number of photons detected in 300.8 ks we calculate

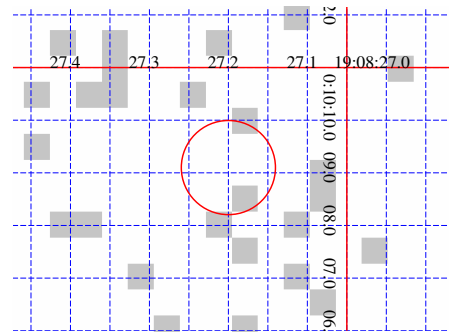


FIG. 1.— Zoom-in on the position of the neutron star SXT 1H 1905+000 in the 0.3–7 keV 300 ks *Chandra* ACIS image. The circle has a radius of 0''.91.

a 95% confidence upper limit on the source count using both the method explained in Gehrels (1986) as well as the method explained in the appendix of Weisskopf et al. (2007). Even though the number of photons falling inside this area is less than 2 we take 2 as the number of detected photons in what follows, to account for the fact that we took the 90% encircled energy radius (not 100%), and to account for the slight smearing that will have occurred due to the alignment of the images introduced by the finite accuracy at which the boresight correction can be determined. Following Weisskopf et al. (2007) we calculate the probability that the background contributes fewer than the 2 photons inside the 90% encircled energy radius. This probability is effectively 0.

From the method of Gehrels (1986), we derive a 95% confidence upper limit on the source count of 6.3 which given the exposure time corresponds to an upper limit on the count rate of 2.1×10^{-5} counts s⁻¹. In the method of Weisskopf et al. (2007) m_T and m_R are defined, corresponding to the number of X-ray photons detected in the Target and Reference apertures of measure Ω_T and Ω_R , respectively. For Ω_T we have taken a circular region with radius of 1'' centered on the source position, as above this gives ≈ 2 counts in the detection region. For Ω_R we have taken an annulus with inner and outer radius of 4''.92 and 39''.36, respectively. We have excluded a weak source from this background area. The size of the areas Ω_T and Ω_R is 3.14 arcsec² and 4790.94 arcsec², respectively (m_T and m_R are 2 and 2750, respectively). The expectation value on the number of source counts for a confidence level of 95% is < 5 counts which corresponds to an upper limit on the count rate of 1.7×10^{-5} counts s⁻¹. In the remainder of the Paper we conservatively use the slightly higher value from the Gehrels (1986) method.

We have used *W3PIMMS*⁴ to estimate 95% confidence limits on the source flux and luminosity in different X-ray bands employing the various models often found for neutron star soft X-ray transients (SXTs) in quiescence. The obtained limits are listed in Table 2. We have estimated the effective temperature at the surface of the neutron star, T_{eff} , and as measured at infinity, T_{eff}^{∞} , as follows: we have used the flux limit obtained for a 0.2 keV black body model as limit for the neutron star atmosphere model in *xspec* version 11.3.2p (Arnaud 1996; Zavlin et al. 1996). Ideally, one would like to use a response and auxiliary response matrix specific for the location of the source on the CCD. However, for the combined observation this is not possible, hence, we have used the standard response files for on-axis ACIS-S observations. Given the distance of 10 kpc, assuming a 1.4 M_{\odot} neutron star with

⁴ available at <http://heasarc.gsfc.nasa.gov/Tools/w3pimms.html>

TABLE 2
UPPER LIMITS TO THE UNABSORBED SOURCE FLUX^a AND LUMINOSITY^b.

Model	$F_{0.5-10\text{keV}} \text{ unabs.}$ $\text{erg cm}^{-2} \text{ s}^{-1}$	$F_{0.01-10\text{keV}} \text{ unabs.}$ $\text{erg cm}^{-2} \text{ s}^{-1}$	$L_{0.5-10\text{keV}}$ $(\frac{d}{10 \text{ kpc}})^2 \text{ erg s}^{-1}$
PL ^c $\Gamma=2.0$	2.0×10^{-16}	4.5×10^{-16}	2.4×10^{30}
BB ^c $T=0.2 \text{ keV}$	1.4×10^{-16}	1.9×10^{-16}	1.6×10^{30}
BB ^c $T=0.1 \text{ keV}$	2.2×10^{-16}	8.8×10^{-16}	2.6×10^{30}

^a Unabsorbed flux (F) is given in the 0.5–10 keV and 0.01–10 keV band. The used interstellar extinction is $2.1 \times 10^{21} \text{ cm}^{-2}$.

^b The luminosity (L) is given for 0.5–10 keV and a distance of 10 kpc.

^c PL stands for power law and BB for blackbody.

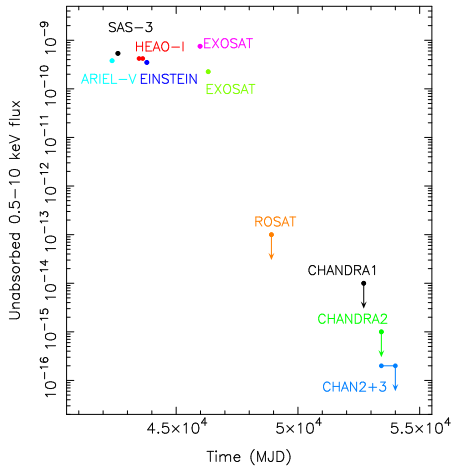


FIG. 2.— The unabsorbed 0.5–10 keV X-ray flux history of 1H 1905+000. The range in dates plotted for the HEAO–I satellite indicates the time span over which the source was detected on multiple occasions by that satellite. The upper limit indicated with “CHAN2+3” has been derived using *Chandra* data from 2005 and 2006 (see Table 1). In order to convert fluxes given in the literature in other X-ray bands to the 0.5–10 keV band we assume the spectrum to be well-represented by an absorbed power law with index 2 (except for the ROSAT and *Chandra* upper limit which were derived assuming a 0.3 and 0.2 keV black body, respectively). Arrows on the data points indicate upper limits to the X-ray flux.

radius of 10 km, a pure Hydrogen, non-magnetic atmosphere, the limits on T_{eff} and T_{eff}^{∞} are $4.6 \times 10^5 \text{ K}$ and $3.5 \times 10^5 \text{ K}$, respectively.

Using the stringent limit on the source luminosity together with detections and limits on the detection of the source obtained at other times we have constructed the long term X-ray lightcurve of 1H 1905+000 (see Fig. 2)⁵. From Fig. 2 it is clear that the source underwent an outburst with a duration of at least 9.9 years (the time between the first and last detection). Using the SAS–3 satellite several type I X-ray bursts were detected (Li et al. 1976 [multiple bursts], Lewin et al. 1976b [5], Lewin et al. 1976a [1]). However, since the persistent flux level was in most cases not quoted only 1 SAS–3 point appears in Fig. 2.

2.2. Magellan optical observations

We obtained Sloan i' -band images using the Magellan Instant Camera (MagIC) instrument mounted on the 6.5 m

⁵ Data for Fig. 2 was taken or derived from Seward et al. (1976) (Ariel–V), Lewin et al. (1976b) (SAS–3), Reid et al. (1980) (HEAO–I), Christian & Swank (1997) (Einstein), Chevalier & Ilovaisky (1990) (EXOSAT, MJD 46316), Gottwald et al. (1995) (EXOSAT, MJD 45982), Voges (1999) (ROSAT), Juett & Chakrabarty (2005) (Chandra1), Jonker et al. (2006) (Chandra2), and this work (Chandra 2+3)

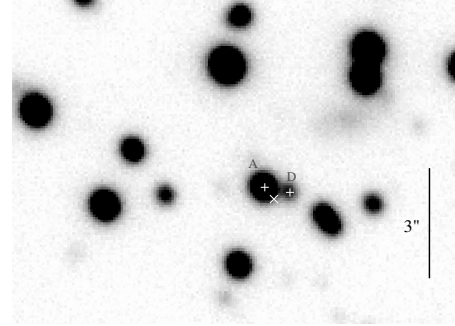


FIG. 3.— Deep, 3×5 minutes integration, Sloan i filter Magellan observation of the field of 1H 1905+000 obtained with the MagIC instrument under a seeing of $0''.4$. The cross indicates the outburst source position. The “+” signs labelled A and D are nearby field stars (labels follow those in Jonker et al. 2006). The vertical bar has a length of $3''$. North is up and East is left.

Magellan–Clay telescope at Las Campanas Observatory. On June 23, 2006 (MJD 53909 UTC), three 300 second exposures were collected between 5:02–5:19 UTC. The observing conditions were excellent with a photometric sky and a seeing of $0''.4$. MagIC delivers a $2.35'$ field of view sampled at $0''.069/\text{pixel}$. Frames were readout in quad amplifier mode, and were debiased and then flatfielded using dithered twilight sky observations.

We astrometrically calibrated the median combined CCD image by matching the positions of stars in the image against those of stars from images presented in Jonker et al. (2006). The latter images were calibrated with respect to the second version of the USNO CCD Astrograph Catalog (Zacharias et al. 2004) to provide a ICRS J2000.0 astrometric frame.

Photometric calibration was performed using images obtained on June 25, 2006 with the 4-m Blanco telescope and its MOSAIC imager at CTIO. A 120s Sloan i' -band image of the field surrounding 1H 1905+000 was obtained under photometric conditions together with observations of the standard star fields PG 1323 and SA 107. These allowed us to perform an absolute magnitude calibration of stars in the proximity of our target. Since we only observed the field of 1H 1905+000 in one filter no color terms have been calculated.

Despite the excellent observing conditions at Magellan, the counterpart of 1H 1905+000 in quiescence is not detected down to a 5σ magnitude limit of $i > 25.3$. A high resolution finder chart is presented in Fig. 3.

3. DISCUSSION

We have obtained a 300 ks-long *Chandra* observation of the field of 1H 1905+000. Using this observation we do not detect the quiescent X-ray counterpart to this neutron star soft X-ray transient. The limit on the source flux depends on the assumed spectral model. For instance, a spectral model of an absorbed power law with index of 2 as observed for weak quiescent neutron star transients and quiescent black hole X-ray transients (Jonker et al. 2004, Kong et al. 2002), gives a 95% confidence upper limit on the 0.5–10 keV source flux of $2.0 \times 10^{-16} \text{ erg cm}^{-2} \text{ s}^{-1}$. Given the upper limit on the source distance of 10 kpc (Chevalier & Ilovaisky 1990, Jonker & Nelemans 2004) this converts to a 0.5–10 keV luminosity limit of $2.4 \times 10^{30} \text{ erg s}^{-1}$. This means that the luminosity of this neutron star SXT is lower than that observed for the weakest black hole SXT A 0620–00 which has for a distance of 1 kpc an unabsorbed quiescent 0.5–10 keV luminosity of $3 \times 10^{30} \text{ erg s}^{-1}$ (Garcia et al. 2001, Kong et al. 2002). Note that some black hole SXTs have not been detected in quies-

cence, and whereas the present upper limit to the luminosity in those cases is well above that derived for 1H 1905+000 one cannot exclude that deeper observations will reveal a lower luminosity than that derived for 1H 1905+000. Nevertheless, from present data the claim that there is evidence for a black hole event horizon from a lower quiescent luminosity in black holes than neutron stars (e.g. Garcia et al. 2001) is unproven and at least does not hold universally.

Scaling of the observed quiescent luminosity with the Eddington luminosity in order to try to normalize the neutron star and black hole systems to the same mass accretion rate is very uncertain. For instance, since an unknown amount of the transferred mass might be lost from the system in the form of a disk wind (e.g. Miller et al. 2006), the relation between the mass transfer and mass accretion rate is not well constrained. This might be especially important for neutron star systems in quiescence if a propellor regime exists (Illarionov & Sunyaev 1975). On the other hand, as shown for instance by Fender (2001), Fender et al. (2003) and Gallo et al. (2006), black holes are producing more powerful jets observable in radio. Matter could also be lost from these systems via these jets, the amount depends on the unknown composition of the jets. Finally, it is unclear whether accretion in low-transfer states proceeds via an advection dominated accretion flow (e.g. ADAF; Narayan & Yi 1995) or via a disk (e.g. Livio et al. 2003).

In deep optical Sloan *i*-band images obtained with the 6.5 m Magellan telescope under excellent conditions (seeing 0.4) we do not detect the optical counterpart to 1H 1905+000. For a distance of 10 kpc the magnitude upper limit of $i > 25.3$ converts into an upper limit on the absolute magnitude of $I = 9.6$ (as in Jonker et al. 2006 we converted the observed outburst N_H from Christian & Swank 1997 to a reddening $A_i = 0.7$ in the Sloan *i* band using the conversion factors given in Rieke & Lebofsky 1985 and Schlegel et al. 1998). This limit implies that the companion star of 1H 1905+000 has a spectral type later than M5 or is a white dwarf as in ultra-compact X-ray binaries. It strengthens the identification of 1H 1905+000 as an ultra-compact X-ray binary (Jonker et al. 2006).

An absorbed thermal neutron star atmosphere spectral model for a distance of 10 kpc gives a limit to the effective temperature at the surface of the neutron star of 4.6×10^5 K (for a neutron star mass and radius of $1.4 M_\odot$ and 10 km, respectively and assuming a pure Hydrogen non-magnetic atmosphere). For such a neutron star this implies an effective

temperature of 3.5×10^5 K at infinity.

A factor in determining the limit on the source flux is the amount of interstellar extinction that is assumed. We have taken the conservative value for the Hydrogen column density of $N_H = 2.1 \times 10^{21} \text{ cm}^{-2}$ from the results of Christian & Swank (1997) who found $N_H = (1.9 \pm 0.2) \times 10^{21} \text{ cm}^{-2}$. Those authors found that the Hydrogen column densities derived for several LMXBs from their spectral fits to Einstein data agree with values found using ROSAT spectra. Besides and related to the N_H , the bolometric correction is important in the conversion of the 0.5–10 keV band limit to a bolometric luminosity limit. E.g. from the upper limit on the effective temperature of a neutron star atmosphere an upper limit to the bolometric luminosity of $10^{31} \text{ erg s}^{-1}$ is determined implying a bolometric correction of ≈ 4 –5. For a power law spectral model with index 2, the bolometric correction would be ≈ 3 (here we have taken the 0.01–100 keV luminosity as a good measure of the bolometric luminosity). In this we again have taken $N_H = 2.1 \times 10^{21} \text{ cm}^{-2}$.

The new deep limit on the quiescent thermal X-ray emission of 1H 1905+000 implies that the neutron star must cool faster than possible with modified URCA processes even for time averaged mass accretion rates as low as $10^{-13} M_\odot \text{ year}^{-1}$ (Jonker et al. 2006), unless the neutron star core is not in a steady state. This would mean that 1H 1905+000 had been in quiescence prior to the ~ 10 year long outburst for ≈ 10 thousand years since the core reaches steady state on such timescales (Colpi et al. 2001, Yakovlev & Pethick 2004). On the other hand, here again one should keep in mind that the relation between the mass transfer and mass accretion rate is not well known especially for quiescent systems. So, it is possible that the time averaged mass transfer rate is larger than $10^{-13} M_\odot \text{ year}^{-1}$ whereas the mass accretion rate onto the neutron star is lower than this.

PGJ acknowledges Ed Brown for useful discussions, support from NASA grant G06-7032X and support from the Netherlands Organisation for Scientific Research. DS acknowledges support through the NASA Guest Observer program as well as a PPARC/STFC Advanced Fellowship. This paper includes data gathered with the 6.5 m Magellan Telescopes located at Las Campanas Observatory, Chile. *Facilities:* Magellan, CXO (ACIS).

REFERENCES

- Arnaud, K. A. 1996, in ASP Conf. Ser. 101: Astronomical Data Analysis Software and Systems V, Vol. 5, 17
- Chevalier, C. & Ilovaisky, S. A. 1990, A&A, 228, 115
- Christian, D. J. & Swank, J. H. 1997, ApJS, 109, 177
- Colpi, M., Geppert, U., Page, D., & Possenti, A. 2001, ApJ, 548, L175
- Fender, R. P. 2001, MNRAS, 322, 31
- Fender, R. P., Gallo, E., & Jonker, P. G. 2003, MNRAS, 343, L99
- Gallo, E., Fender, R. P., Miller-Jones, J. C. A., Merloni, A., Jonker, P. G., Heinz, S., Maccarone, T. J., & van der Klis, M. 2006, MNRAS, 370, 1351
- Garcia, M. R., McClintock, J. E., Narayan, R., Callanan, P., Barret, D., & Murray, S. S. 2001, ApJ, 553, L47
- Gehrels, N. 1986, ApJ, 303, 336
- Gottwald, M., Parmar, A. N., Reynolds, A. P., White, N. E., Peacock, A., & Taylor, B. G. 1995, A&AS, 109, 9
- Heinke, C. O., Jonker, P. G., Wijnands, R., & Taam, R. E. 2006, ArXiv Astrophysics e-prints
- Illarionov, A. F. & Sunyaev, R. A. 1975, A&A, 39, 185
- Jonker, P. G., Bassa, C. G., Nelemans, G., Juett, A. M., Brown, E. F., & Chakrabarty, D. 2006, MNRAS, 368, 1803
- Jonker, P. G., Galloway, D. K., McClintock, J. E., Buxton, M., Garcia, M., & Murray, S. 2004, MNRAS, 354, 666
- Jonker, P. G. & Nelemans, G. 2004, MNRAS, 354, 355
- Juett, A. M. & Chakrabarty, D. 2005, ApJ, 627, 926
- Kong, A. K. H., McClintock, J. E., Garcia, M. R., Murray, S. S., & Barret, D. 2002, ApJ, 570, 277
- Lewin, W. H. G., Doty, J., Hoffman, J. A., & Li, F. K. 1976a, IAU Circ., 2984, 2
- Lewin, W. H. G., Li, F. K., Hoffman, J. A., Doty, J., Buff, J., Clark, G. W., & Rappaport, S. 1976b, MNRAS, 177, 93P
- Li, F., Lewin, W. H. G., & Doxsey, R. 1976, IAU Circ., 2983, 1
- Livio, M., Pringle, J. E., & King, A. R. 2003, ApJ, 593, 184
- Miller, J. M., Raymond, J., Fabian, A., Steeghs, D., Homan, J., Reynolds, C., van der Klis, M., & Wijnands, R. 2006, Nature, 441, 953
- Murray, S. S. e. a. 2005, ApJS, 161, 1
- Narayan, R. & Yi, I. 1995, ApJ, 452, 710
- Reid, C. A., Johnston, M. D., Bradt, H. V., Doxsey, R. E., Griffiths, R. E., & Schwartz, D. A. 1980, AJ, 85, 1062
- Rieke, G. H. & Lebofsky, M. J. 1985, ApJ, 288, 618
- Schlegel, D. J., Finkbeiner, D. P., & Davis, M. 1998, ApJ, 500, 525

- Seward, F. D., Page, C. G., Turner, M. J. L., & Pounds, K. A. 1976, MNRAS, 175, 39P
- Tomsick, J. A., Gelino, D. M., & Kaaret, P. 2005, ApJ, 635, 1233
- Voges, W. e. a. 1999, A&A, 349, 389
- Weisskopf, M. C., Wu, K., Trimble, V., O'Dell, S. L., Elsner, R. F., Zavlin, V. E., & Kouveliotou, C. 2007, ApJ, 657, 1026
- Wijnands, R., Homan, J., Heinke, C. O., Miller, J. M., & Lewin, W. H. G. 2005, ApJ, 619, 492
- Yakovlev, D. G. & Pethick, C. J. 2004, ARA&A, 42, 169
- Zacharias, N., Urban, S. E., Zacharias, M. I., Wycoff, G. L., Hall, D. M., Monet, D. G., & Rafferty, T. J. 2004, AJ, 127, 3043
- Zavlin, V. E., Pavlov, G. G., & Shibanov, Y. A. 1996, A&A, 315, 141